

64288

N92-19123

# Chapter 3A

## Natural Cycles, Gases

A. R. Douglass, C. H. Jackman  
R. B. Rood, A. C. Aikin, and R. S. Stolarski  
National Aeronautics and Space Administration  
Goddard Space Flight Center  
Greenbelt, MD

M. P. McCormick  
National Aeronautics and Space Administration  
Langley Research Center  
Hampton, VA

D. W. Fahey  
National Oceanic and Atmospheric Administration  
Aeronomy Laboratory  
Boulder, CO

NC999967

ND 210491

NJ920944

32  
MEMORANDUM CLASS

PRECEDING PAGE BLANK NOT FILMED

## ABSTRACT

The major gaseous components of the exhaust of stratospheric aircraft are expected to be the products of combustion ( $\text{CO}_2$  and  $\text{H}_2\text{O}$ ), odd nitrogen ( $\text{NO}$ ,  $\text{NO}_2$ ,  $\text{HNO}_3$ ), and products indicating combustion inefficiencies ( $\text{CO}$  and total unburned hydrocarbons, THC). The species distributions are produced by a balance of photochemical and transport processes. A necessary element in evaluating the impact of aircraft exhaust on the lower stratospheric composition is to place the aircraft emissions in perspective within the natural cycles of stratospheric species. Following are a description of mass transport in the lower stratosphere and a discussion of the natural behavior of the major gaseous components of the stratospheric aircraft exhaust. The roles of soot and  $\text{SO}_2$  are discussed in the next chapter.

## MASS TRANSPORT IN THE LOWER STRATOSPHERE

The natural cycle of long-lived species is dominated by transport. A qualitative picture of the zonal and time averaged stratospheric transport was proposed by Brewer (1) to explain the observed sharp decrease in water vapor at the middle latitude tropopause. In this description, air rises in the tropics and is transported poleward and downward at middle and high latitudes. Transport from the troposphere to the stratosphere is limited to the tropics, where the tropopause temperatures are coldest. The temperatures are cold enough to produce saturation with respect to ice, and the ice particles fall. This freeze-dry mechanism thus provides a limit to the amount of water vapor that is allowed to enter the stratosphere. Although the water vapor measurements are even lower than would be allowed by the average temperatures of the tropical tropopause, indicating that the actual mechanism by which air enters the stratosphere is more complicated, this qualitative picture of mass transport is consistent with measurements of other species. Dobson (2) pointed out that this concept of a circulation (the Brewer-Dobson circulation) is consistent with ozone observations, which show the highest ozone concentrations in the polar stratosphere, away from the tropical source region. Observations of species such as  $\text{N}_2\text{O}$ , which have tropospheric sources and significant loss processes only in the mid to upper stratosphere, are also compatible with the Brewer-Dobson circulation.

Even though transport processes in the atmosphere are three-dimensional (3-D), two-dimensional (2-D) formulations provide a convenient conceptual framework to discuss global processes. Furthermore, 2-D models remain at the center of assessment calculations because they are computationally manageable. On the most basic level, stratospheric transport can be viewed as advection by a large-scale mass transport circulation such as the Brewer-Dobson circulation discussed in the previous paragraph. Coupled with this advective circulation is large-scale quasi-horizontal mixing caused by Rossby waves. The general characteristics of these two transport mechanisms are lucidly discussed by Mahlman (3).

Even though the 2-D framework does offer a useful format in which to discuss global transport processes, the mechanics of casting the 3-D circulation into two dimensions are not straightforward. Because of this, the best determination of the 2-D advective transport is not clear. The simplest idea is to use geometric zonal means about latitude circles to calculate a meridional and vertical velocity. This sort of averaging, termed the Eulerian mean, yields a meridional flow that is not like the Brewer-Dobson circulation. This difference between the expected mass flow and the Eulerian mean arises because of a compensating circulation that is driven by the planetary (Rossby) waves. This compensating circulation is a practical manifestation of the non-interaction theorem which states that planetary waves have no effect on the mean flow in the absence of transience, dissipation, or nonlinearity. While these constraints are never strictly met, there is a large compensation between the waves and the Eulerian mean flow, and hence, the advective mass circulation is a small residual that must be derived from two larger, competing terms.

34

Alternatives to the Eulerian mean have proven very effective in recasting the 2-D problem. These are discussed in some detail in chapter 6 of *Atmospheric Ozone 1985* (4). Theoretically, the most useful framework has proven to be the Lagrangian mean circulation. Averages in the Lagrangian mean follow wavy material tubes, and the Lagrangian mean velocity tracks this material tube. In the instance of the Eulerian circulation mentioned above, it is found that the Lagrangian mean circulation associated with planetary waves is an advective circulation directed opposite to the Eulerian zonal mean and with slightly greater magnitude. Dunkerton (5) showed that the Brewer-Dobson view of mass transport should be interpreted as a Lagrangian mean. Though the concept of the Lagrangian mean is useful theoretically, the necessity of averaging over wavy material tubes makes a Lagrangian mean model impractical.

Other estimates of the mean meridional circulation include the transport circulation, the diabatic circulation, and the residual circulation. Of these estimates, the residual circulation is the most frequently used because it is relatively simple to calculate from transformed Eulerian mean equations. These equations are derived by consideration of the large-scale equations of motion and combining the heat flux term with the Eulerian advective velocity, to yield a residual advective velocity. This procedure effectively captures some, but not all, of the characteristics of the noninteraction theorem. Comparisons of the Lagrangian mean and residual circulations for simple systems were discussed by Rood and Schoeberl (6), who showed differences between the two circulations on the order of 30%.

Residual circulation models have had considerable success in their representations of stratospheric constituent distributions. Calculations for species such as  $N_2O$  and column  $O_3$ , using both Eulerian mean and residual circulation 2-D models, are in qualitative agreement with available global measurements (7). The fact that the residual circulation does offer an approximation to the mass flow of the atmosphere is useful in the discussions below. The transport effects of the planetary waves, "diffusive transport," constitute a complicated issue that will not be considered further here. Both chapter 6 of *Atmospheric Ozone 1985* (4) and Andrews et al. (8) offer more detailed discussions of transport processes.

A crucial issue for the High-Speed Research Program (HSRP) is the transport from the stratosphere to the troposphere. Exchange processes are discussed in detail in chapter 5 of *Atmospheric Ozone 1985* (4) and they are considerably more complicated than can be represented by 2-D transport descriptions. Accurate representations of convective processes and subplanetary scale eddies are essential ingredients of stratosphere/troposphere exchange. Three-dimensional models have not effectively dealt with these problems. The data record has only begun to identify and address the mechanisms of exchange. Aside from tropical convection, it is very likely that significant mass exchange is driven by quasi-horizontal eddies in latitudinally and longitudinally confined regions.

In a time-averaged global domain, the residual circulation can be used to provide at least a crude estimate of the mass exchange between the stratosphere and the troposphere. This can then be used to estimate stratospheric residence time and, hence, the relative perturbation to the background field caused by a pollutant. Consider a stratospheric volume bounded below by the tropopause, above by the 50 mb surface, and extending in latitude ( $\phi$ ) from 30°N to 90°N. The vertical mass flux,  $F$ , is calculated according to

$$F = 2\pi r_e^2 \int_{\phi = 30^\circ N}^{\phi = 90^\circ N} \rho_0 w^* d(\sin\phi) \quad (1)$$

where  $r_e$  is the radius of the earth (cm),  $\rho_0$  is the density ( $\text{g cm}^{-3}$ ), and  $w^*$  is the residual vertical velocity ( $\text{cm s}^{-1}$ ) across the tropopause or the 50-mb surface. As noted previously, the estimate of mass exchange calculated using the residual circulation is incomplete because eddy transports are not included. There is additional uncertainty because the residual circulation is determined from the heating rate calculations in the lower stratosphere. The heating and cooling terms are nearly balanced, and the net heating from which the residual circulation is derived is small. Sensitivity of calculations to small changes in the heating rates is considered by Jackman et al. (9).

The value of  $F_{\text{trop}}$  is estimated to be  $1.4 - 2.4 \times 10^{17} \text{ kg yr}^{-1}$ . This estimate is based on an evaluation of two residual circulations, RC1 from the NASA/Goddard 2-D model (10) and RC2 from the model discussed by Shia et al. (11). These may be compared with the estimate of Holton (12) for the mass flux through the 100-mb surface of  $1.3 \times 10^{17} \text{ kg yr}^{-1}$ , and the minimum estimate of  $1 \times 10^{17} \text{ kg yr}^{-1}$  given by Robinson (13). An extreme upper limit of  $5.8 \times 10^{17} \text{ kg yr}^{-1}$  is obtained using a circulation RC3, which has larger values of the diabatic heating in the lower stratosphere. This is considered an extreme limit because of poor agreement between the annual variation of total ozone calculated using the RC3 circulation and Total Ozone Mapping Spectrometer (TOMS) measurements (9).

The downward vertical mass flux across the 50-mb surface is about  $9 \times 10^{16} \text{ kg yr}^{-1}$  for RC1, RC2, and RC3. Because the vertical flux out of the layer exceeds the vertical flux into the layer, there must be poleward horizontal transport into the region across  $30^\circ\text{N}$ . The total mass in this region is about  $21 \times 10^{16} \text{ kg}$ ; the outflow values cited previously imply a turnover time of 0.9 to 1.5 years for this northern-hemisphere segment of the lower stratosphere.

This simple model may be used for first-order estimates of the buildup of pollutants in the lower stratosphere resulting from aircraft exhaust. For any species with a continuity equation may be written for the stratospheric volume described in the previous section

$$\partial\chi/\partial t = [F_{\text{in}} \chi_i - F_{\text{out}} \chi] / M + P/M - L\chi \quad (2)$$

where  $F_{\text{in}}$  and  $F_{\text{out}}$  are the annual mass fluxes of air into and out of the region,  $\chi_i$  is the mass mixing ratio of the incoming air-mass flux ( $F_{\text{in}}$ ),  $M$  is the air mass of the stratospheric volume (kg),  $P$  is the total photochemical production rate ( $\text{kg s}^{-1}$ ), and  $L$  is the averaged loss frequency ( $\text{s}^{-1}$ ). In the presence of aircraft, there is an additional source ( $P_{\text{aircraft}}$ ). At steady-state,  $\partial\chi/\partial t = 0$ , and the additional  $\chi$  associated with the aircraft source is

$$\chi_{\text{aircraft}} = P_{\text{aircraft}} / (F_{\text{out}} + LM) \quad (3)$$

An upper limit estimate to  $\chi_{\text{aircraft}}$  can be made by dropping the chemical term ( $LM$ ). For fuel use of  $7.7 \times 10^{10} \text{ kg yr}^{-1}$  and the outflow estimated above,

$$\chi_{\text{aircraft}} = (7.7 \times 10^7 \text{ EI}) / (1.4-2.4 \times 10^{17}), \quad (4)$$

where EI is the emission index ( $\text{g/kg fuel}$ ). The conversion to volume mixing ratios, summarized in Table 1, is performed by scaling with the ratio of 29 over the mean molecular weight of the emitted species.

**Table 1.** Approximate Perturbations  $\chi'$  to Stratospheric Trace Gases  
( $7.7 \times 10^{10}$  kg of fuel/year)

Species	EI (gm/kg fuel)	Molecular weight	Background	Perturbation
CO <sub>2</sub>	3100	44	350 ppmv	0.7 - 1.2 ppmv
CO	5	28	10 - 50 ppbv	1.7 - 1.8 ppbv
H <sub>2</sub> O	1200	18	2 - 6 ppmv	0.6 - 1.1 ppmv
NO <sub>y</sub>	15	46	2 - 16 ppbv	3.0 - 5.2 ppbv

### CARBON DIOXIDE (CO<sub>2</sub>)

Carbon dioxide is a product of combustion and one of the major components of aircraft exhaust. The EI for CO<sub>2</sub> (chapter 1) is roughly 3100 g of CO<sub>2</sub> per kg of fuel. Carbon dioxide is chemically inert in the lower stratosphere, i.e., there are no significant photochemical production or loss processes. Measurements of the mixing ratio profile indicate little height dependence (14,15), which is expected in view of the steadily increasing tropospheric values. Current tropospheric measurements indicate a volume mixing ratio of about 350 ppmv (16). Assuming that this value is representative of the lower stratosphere, there are approximately  $1 \times 10^{14}$  kg in the bounded area described in the previous section. For an estimated fleet fuel usage of  $7.7 \times 10^{10}$  kg/yr, this corresponds to the source of CO<sub>2</sub> of  $2 \times 10^{11}$  kg yr<sup>-1</sup>. The average increase in CO<sub>2</sub> over this volume is 0.7 to 1.2 ppmv (Table 1), less than 1% of the background level.

### CARBON MONOXIDE (CO)

Carbon monoxide reacts in the lower stratosphere with the hydroxyl radical. The photochemical lifetime, taken from the NASA/Goddard 2-D model (10), is given in Figure 1. Although short lived in the upper stratosphere, the lifetime of CO in the lower stratosphere (1 to 4 years) is comparable to its turnover time (1 to 3 years). Carbon monoxide provides a measure of combustion inefficiency, and the estimated EI values are all less than 5 g of CO per kg of fuel. Although this source of CO ( $< 3.8 \times 10^8$  kg/yr for  $7.7 \times 10^{10}$  kg of fuel) may be comparable to the natural source of CO (about  $6.5 \times 10^8$  kg/yr for the bounded region, largely a result of methane oxidation), the long lifetime indicates that the perturbation will be controlled by mass flow through the region. If chemical effects are neglected, the expected perturbation to the volume mixing ratio is less than 2 ppbv, compared with the natural level in the lower stratosphere of 10 to 50 ppbv (Table 1).

### WATER VAPOR (H<sub>2</sub>O)

Water vapor is a product of combustion and an important component of aircraft exhaust. The normal H<sub>2</sub>O mixing ratios in the lower stratosphere are low (3-5 ppmv), as will be discussed further in this section. The perturbation is estimated to be 0.6 - 1.1 ppmv, which is significant compared with the background values (Table 1). Because of its importance to the lower stratosphere, a more thorough examination of available data is warranted. Water vapor is the major source for odd hydrogen radicals in the stratosphere, generated through reactions with excited atomic oxygen O(1D). Odd hydrogen reactions contribute to the ozone loss throughout

the stratosphere and are most frequent in the lower stratosphere and mesosphere (17). They also modify the ozone destruction efficiency of odd nitrogen and odd chlorine compounds, making chlorine more effective and nitrogen less effective. The amount of water vapor incorporated in aerosols is potentially critically important for the efficiency of heterogeneous reactions (18,19,20), which may directly affect the balance of odd nitrogen and odd chlorine species in the lower stratosphere. The formation of polar stratospheric clouds, either nitric acid trihydrate or ice clouds, depends on the stratospheric temperature and on the amount of water vapor available. The most important photochemical process that affects stratospheric water is oxidation of methane ( $\text{CH}_4$ ), which produces about half of the water vapor in the upper stratosphere. A detailed discussion of the photochemistry of  $\text{CH}_4$ , the production of stratospheric  $\text{H}_2\text{O}$ , and the role of molecular hydrogen ( $\text{H}_2$ ) is provided by LeTexier et al. (21).

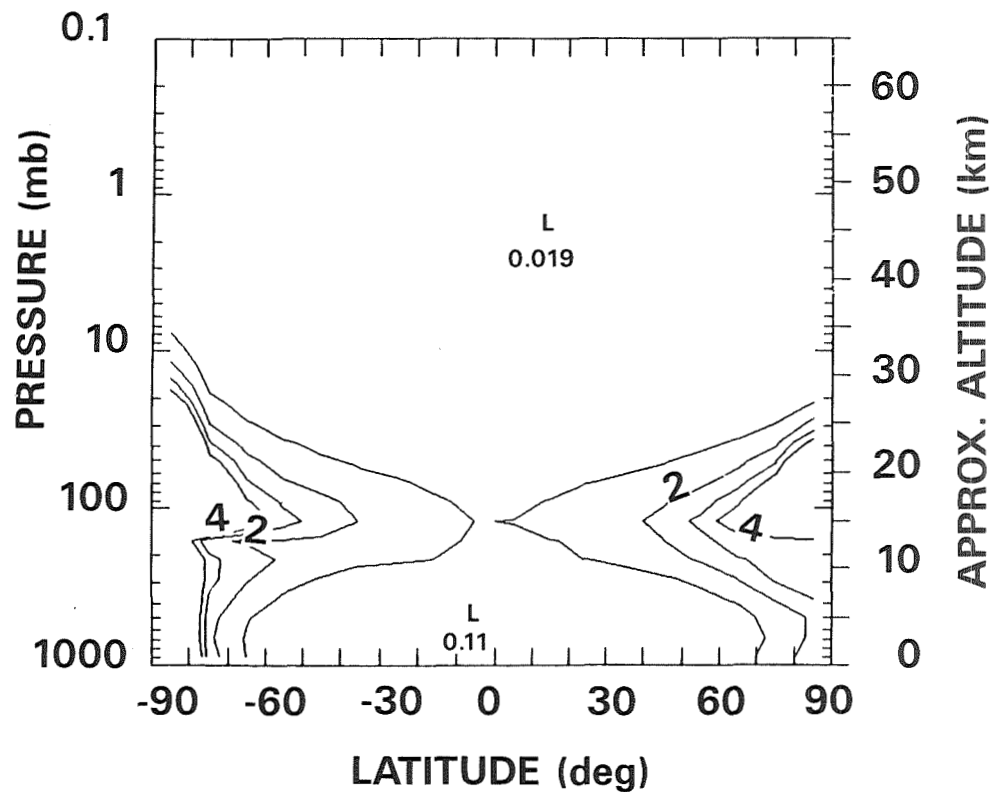


**Figure 1.** The photochemical lifetime of CO (years) (March) taken from the NASA/GSFC 2-D model.

Water vapor measurements have long been considered a useful indicator of stratospheric transport. Early sonde measurements of the water vapor profile showed a rapid decrease in the mixing ratio profile above the midlatitude tropopause. The measured values were substantially lower than the tropopause saturation mixing ratio at middle latitudes. The Brewer-Dobson circulation was proposed as an explanation for these observations (1,2). Rising air enters the stratosphere only in the tropics, where there is rising motion, and is transported poleward and downward at middle and high latitudes. The stratospheric water vapor mixing ratio is limited by the cold temperatures of the tropical tropopause. More recent measurements (22) have demonstrated the existence of a hygropause, a minimum in water vapor mixing ratio above the tropopause at 19-22 km between 30°N and 30°S.

Various techniques have been applied to the measurement of stratospheric water. These were reviewed by the WMO in 1986 (4). Although there are measurements of individual profiles that use assorted techniques, until recently balloon-borne frost point hygrometer measurements provided the most complete picture of annual behavior. In Figure 2, taken from Mastenbrook and Oltmans (23), the annual variation of water vapor (mass mixing ratio) is given for 1964-76 at Washington, DC (39°N, 77°W). The annual cycle near 50-100 mb is much weaker compared with the annual cycle near 150 mb. Similar behavior is seen for a data set taken at Boulder, CO (40°N, 105°W) for 1981-89 (Figure 3). In the lower stratosphere, near 70 mb, there is still a seasonal cycle, with a maximum value in the second half of the year. The seasonal motion of the tropopause is clearly visible, reaching a maximum altitude (i.e., highest H<sub>2</sub>O) in August to September. The increase in mixing ratio with altitude indicates the production of H<sub>2</sub>O from CH<sub>4</sub>.

The first global measurements of water vapor were provided by the Limb Infrared Monitor of the Stratosphere (LIMS) experiment for the period November 1978 through May 1979 (24). The vertical resolution of the measurements is 4 km. At 50 mb, there is a pronounced latitudinal gradient, as shown in Figure 4, consistent with upward motion in the tropics. The gradient is much weaker at 10 mb. The magnitude of the annual variation is consistent with that derived from the frost point hygrometer measurements shown in Figures 2 and 3. Zonal mean profiles for each month during the LIMS period are given in Figure 5(a-g). These measurements are in general agreement with rising motion in the tropics, downward motion at the high latitudes, and a high-altitude source.

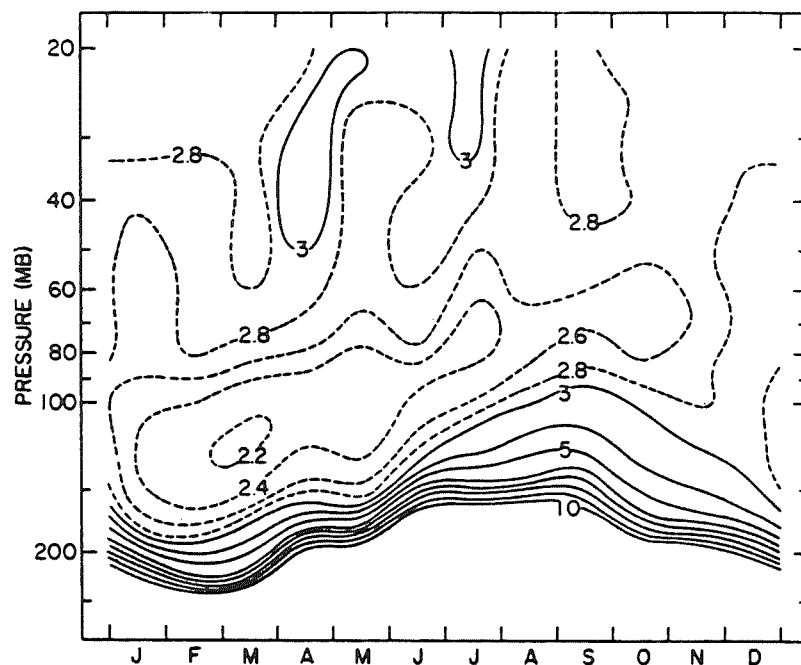


**Figure 2.** Annual variation of stratospheric water vapor (mass mixing ratio) based on balloon-borne frost point hygrometer measurements at Washington, DC, for the period 1974-76 (Mastenbrook and Oltmans [23]).

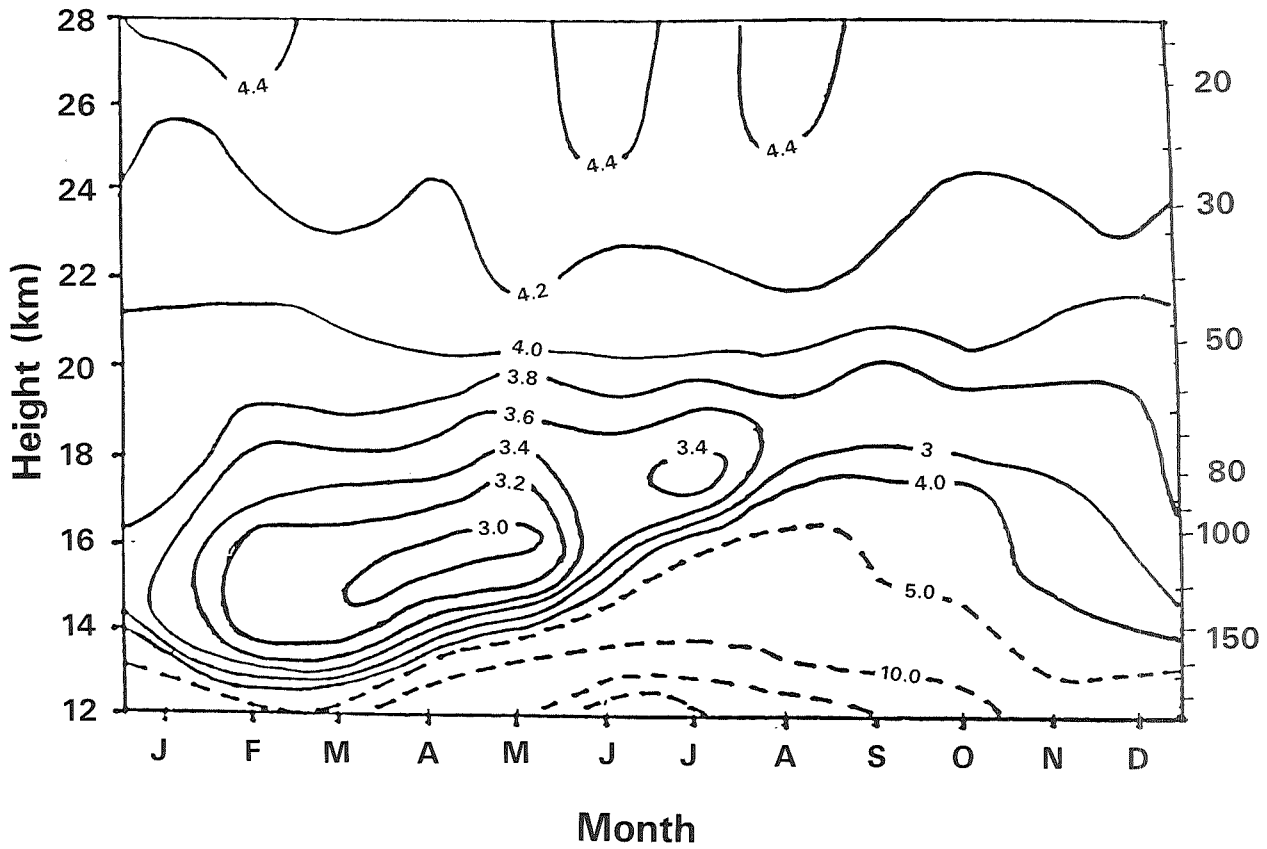


Figure 3. Annual variation of stratospheric water vapor (volume mixing ratio) based on balloon-borne frost point hygrometer measurements at Boulder, CO for the period 1981-89.

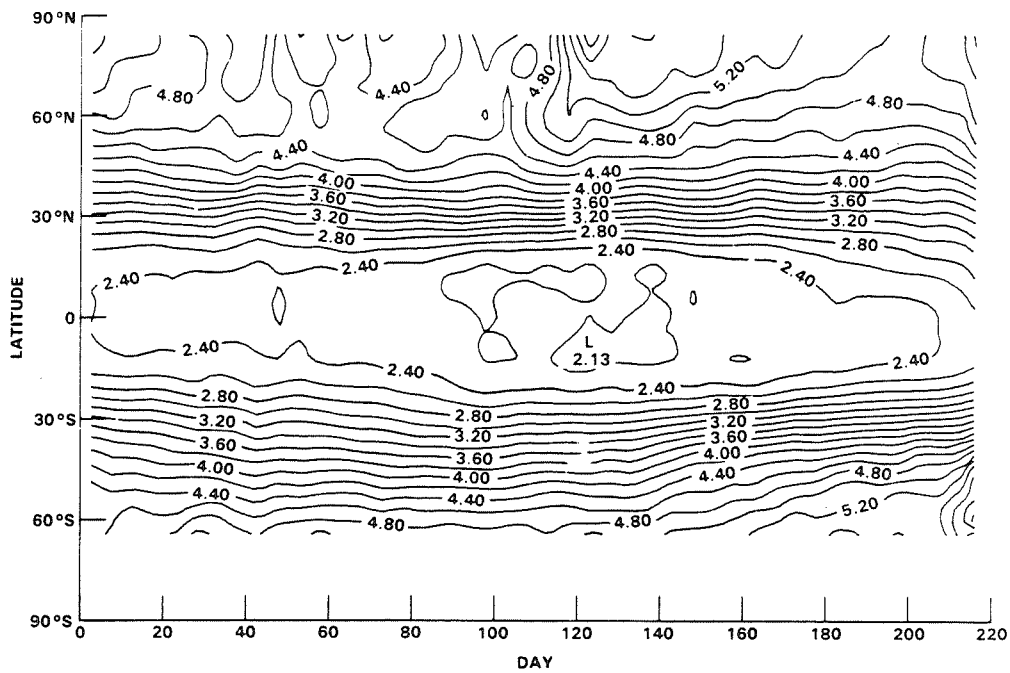
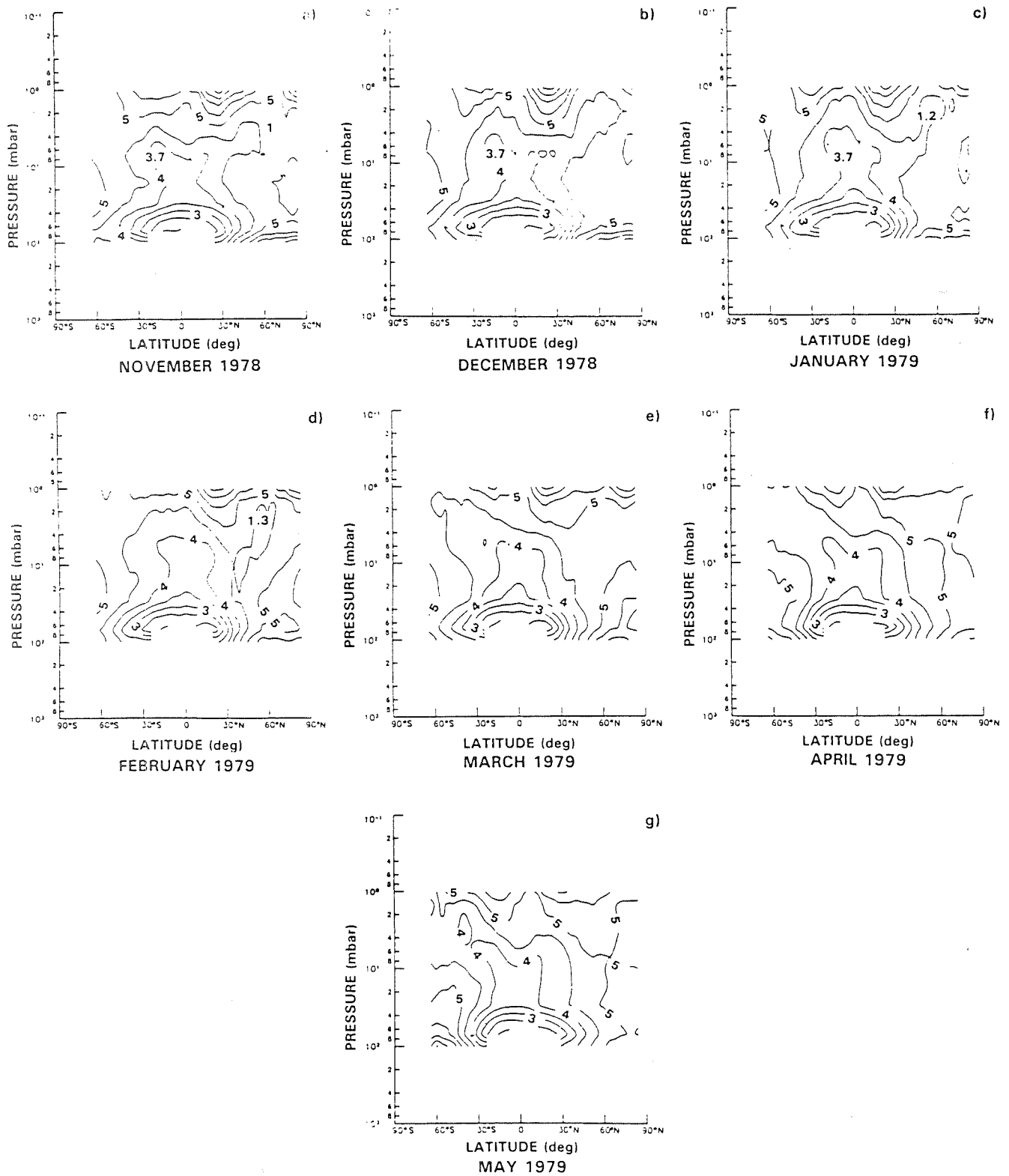


Figure 4. LIMS water vapor latitude versus time cross section at 50 mb (0.25-ppmv intervals, 5-day means).





**Figure 5.** LIMS monthly zonal mean water vapor pressure versus latitude cross sections for (a) November and (b) December 1978 and (c) January, (d) February, (e) March, (f) April, and (g) May 1979 (0.5-ppmv contour intervals).

The Stratospheric Aerosol and Gas Experiment (SAGE II) aboard the Earth Radiation Budget Satellite was launched in 1984. The vertical resolution of this solar occultation instrument is 1 km. The SAGE II measurements provide a much longer data record than previously available, and furnish a picture of seasonal and year-to-year variability in the upper troposphere and stratosphere over much of the globe. The water vapor data, validation studies, and initial results are discussed by Rind et al. (25,26), Chiou et al. (27), Chu et al. (28), Larsen et al. (29), McCormick et al. (30), and Oltmans et al. (31). Validation studies conducted after the Sage II launch have included comparisons with correlative balloon-borne frost point hygrometer and a limited number of aircraft Lyman-alpha flights. Figures 6(a) and 6(b) are examples of comparisons with frost point measurements over Boulder and Lyman-alpha measurements over southern high latitudes, respectively.

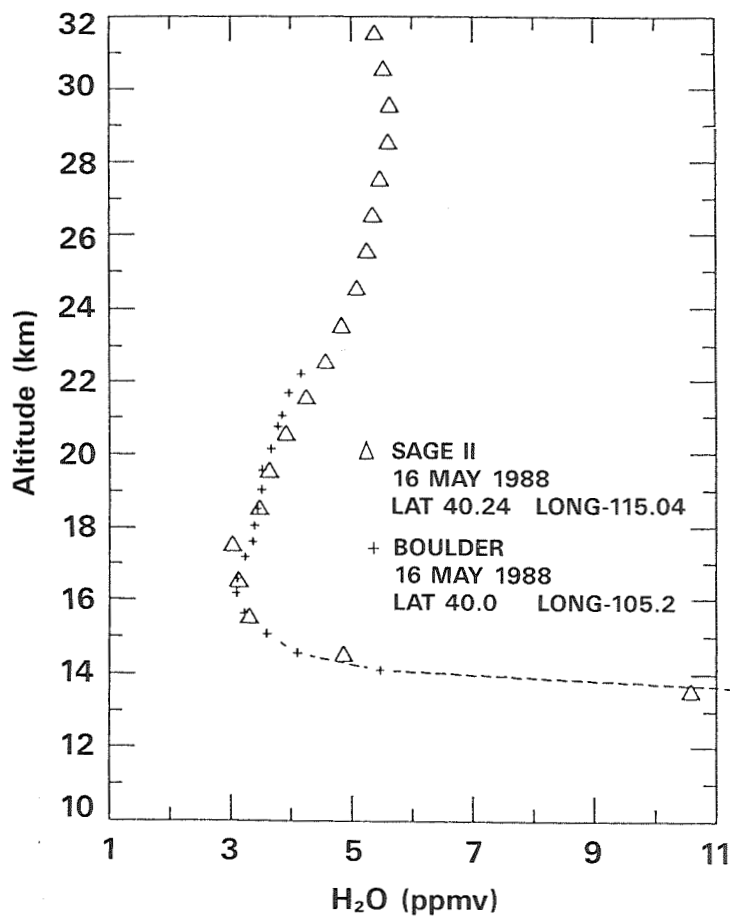
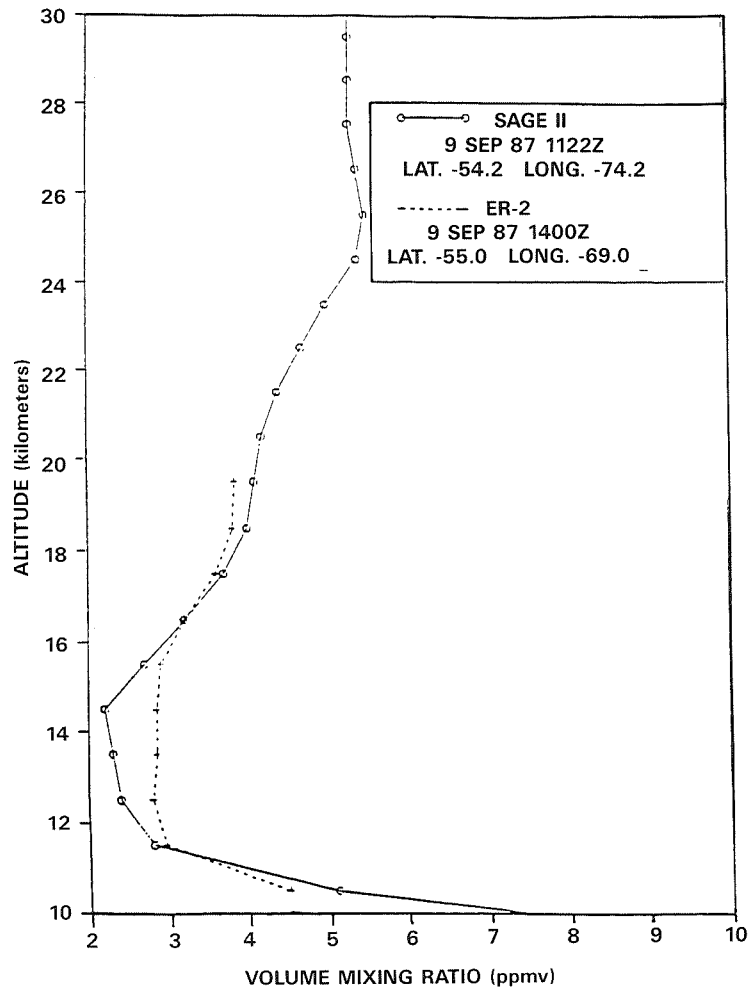


Figure 6(a). Comparison of SAGE II measurements with frost point hygrometer measurements near Boulder CO.



**Figure 6(b).** Comparison of SAGE II measurements with aircraft Lyman-alpha measurements at southern middle latitudes.

A time series of the average water-vapor-mixing ratio between 30° N and 40° N is given in Figure 7. There is excellent agreement between the seasonal pattern in the SAGE II data and the 7 years of balloon measurements made over Boulder (Figure 3). Both show a minimum in early winter near the altitude range 14-15 km. The minimum has its lowest value in March, and thereafter weakens and shifts to higher altitudes. The balloon data show that the magnitude of the seasonal variation near 100 mb at mid to high latitudes is smaller than might be expected based on the LIMS data, but the phases of the variations are similar.

The altitude-latitude cross section of SAGE II water vapor mixing ratios are given for May 1987 in Figure 8. The SAGE measurements are also consistent with the Brewer-Dobson view of mass transport and a high altitude source. These measurements compare well with the measurements in Figure 5(g) from the LIMS instrument.

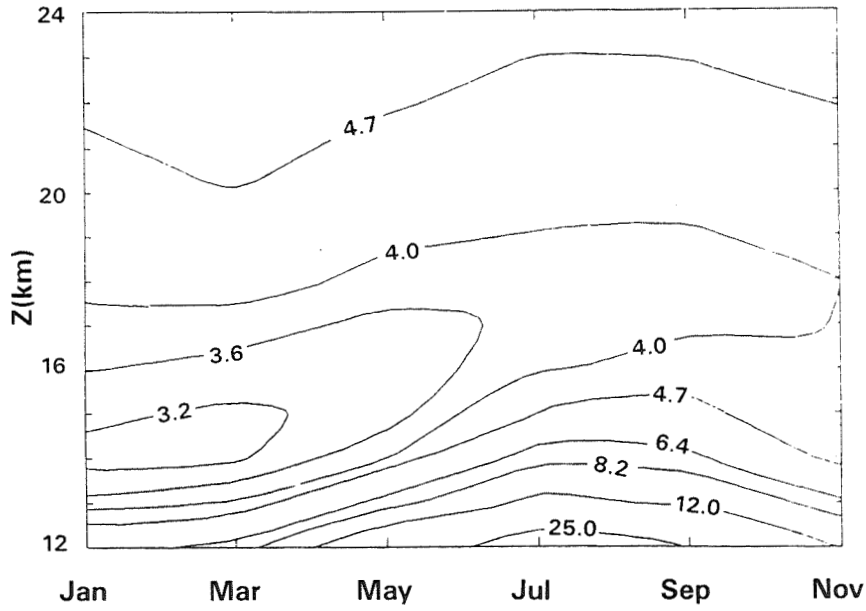


**Figure 7.** Annual variation of stratospheric water vapor (volume mixing ratio, ppmv) from SAGE II measurements, 1987, 30°N-40°N.

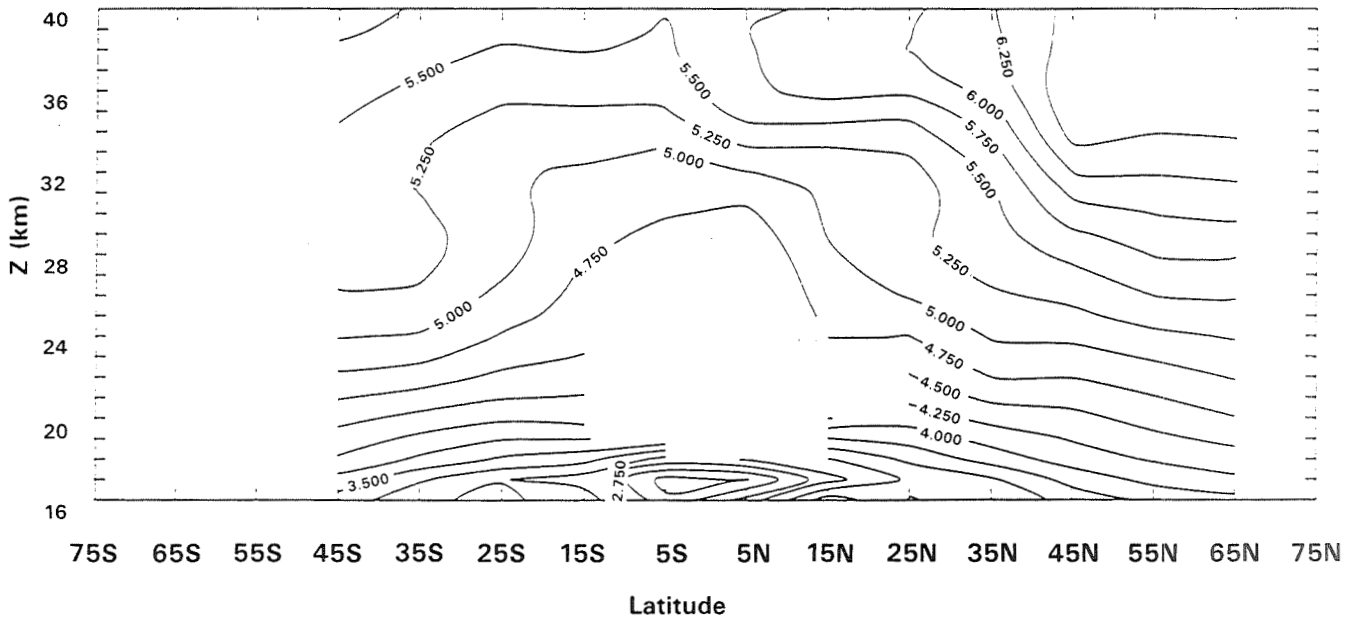


**Figure 8.** The latitude-altitude distribution of SAGE II measurements of water vapor (volume mixing ratio, ppmv) for May 1987.

## ODD NITROGEN

Odd nitrogen species (primarily NO and NO<sub>2</sub>) constitute an important trace component of aircraft exhaust. The anticipated perturbation to total odd nitrogen is significant compared with the normal background values, to be discussed later. Odd nitrogen species (total odd nitrogen = NO<sub>y</sub> = N+NO+NO<sub>2</sub>+NO<sub>3</sub>+2\*N<sub>2</sub>O<sub>5</sub>+HNO<sub>3</sub>+ HNO<sub>4</sub>+ClONO<sub>2</sub>; NO<sub>x</sub> = NO+NO<sub>2</sub>+NO<sub>3</sub>) are extremely important to the stratospheric ozone balance. Odd nitrogen is computed to account for about 50% of the total ozone loss below 40 km and between 60 and 90% of the ozone loss in the lower stratosphere (17). Although there are many measurements of individual odd nitrogen species, there are few measurements that can be interpreted as presenting a global picture of total odd nitrogen. The natural cycles must be derived from a combination of models and data. Following is a discussion of sources of stratospheric odd nitrogen, including nitrous oxide oxidation, galactic cosmic rays (GCRs), lightning (with upflux from the troposphere to the stratosphere), solar proton events (SPEs), relativistic electron precipitations (REPs), and dissociation of N<sub>2</sub> in the thermosphere (with downflux through the mesosphere to the stratosphere). Nuclear explosions, specifically above-ground detonations with energies above 1 megaton, also can produce large amounts of odd nitrogen in the stratosphere. The only loss processes for total odd nitrogen are recombination of N and NO in the upper stratosphere and mesosphere, and transport to the troposphere.

### Natural Sources of Odd Nitrogen

The major source of stratospheric odd nitrogen results from nitrous oxide oxidation (N<sub>2</sub>O + O[<sup>1</sup>D] → NO + NO); several groups have computed globally averaged annual production rates (32-36). An example of the model computation of the odd nitrogen production rate from the oxidation of N<sub>2</sub>O for March (dashed line) is given in Figure 9. This production rate was taken from a 2-D model computation wherein the N<sub>2</sub>O levels were constrained by stratospheric and mesospheric sounder (SAMS) measurement, and the O<sub>3</sub> levels were constrained by measurement from the solar backscatter ultraviolet (SBUV) data [see Figure 9a, Jackman et al. (36)]. The global annually averaged production of odd nitrogen from this source is about 2.6 × 10<sup>34</sup> molecules yr<sup>-1</sup> and is compared with other odd nitrogen sources in Table 2.

**Table 2.** Comparison of Odd Nitrogen Sources and Sinks in the Stratosphere

Source	Magnitude (10 <sup>33</sup> molecules yr-1)
Nitrous oxide oxidation N <sub>2</sub> O + O( <sup>1</sup> D) → NO + NO	26.
Galactic cosmic rays	3.7 (solar minimum) 2.7 (solar maximum)
Lightning	11.
Solar proton events	1.5 (maximum in 1972)
Thermospheric downflux	?
Relativistic electron precipitations	?
Nuclear explosions	24. (1961 & 1962 nuclear tests)
High speed civil transport planes	14. (emission index = 15)
SINK	
Reforming of molecular nitrogen N + NO → N <sub>2</sub> + O	8.4
Transport to the troposphere	32.

Galactic cosmic rays produce odd nitrogen in the lower stratosphere and upper troposphere. The earth's magnetic field influences the GCRs to a certain extent, such that more GCRs affect the atmosphere at higher geomagnetic latitudes. Galactic cosmic rays produce odd nitrogen through dissociation or dissociative ionization processes in which  $N_2$  is converted to  $N(4S)$ ,  $N(2D)$ , or  $N^+$  (33,37,38). Rapid chemistry is initiated after  $N_2$  dissociation, and most of the atomic nitrogen is rapidly converted to  $NO$  and  $NO_2$ . The GCR mean production rate of odd nitrogen [solid line, taken from Figure 13 of Jackman et al. (36)] is compared with the oxidation of  $N_2O$  source in Figure 9. A solar cycle variation is apparent in the GCR flux. The stratospheric component of the odd nitrogen production is estimated to be a maximum of  $3.7 \times 10^{33}$  molecules  $yr^{-1}$  during solar minimum and a minimum of  $2.7 \times 10^{33}$  molecules  $yr^{-1}$  during solar maximum (33).

Natural production of odd nitrogen is dominated in the middle and upper stratosphere by  $N_2O$  oxidation and in the lower stratosphere at the higher latitudes by the GCRs. Since the odd nitrogen family has a lifetime of months in the middle and lower stratosphere, transport of odd nitrogen created at higher altitudes and lower latitudes is significant, and thus the GCR source of odd nitrogen has been computed to increase odd nitrogen in the lower stratosphere at high latitudes by only about 10% (37).

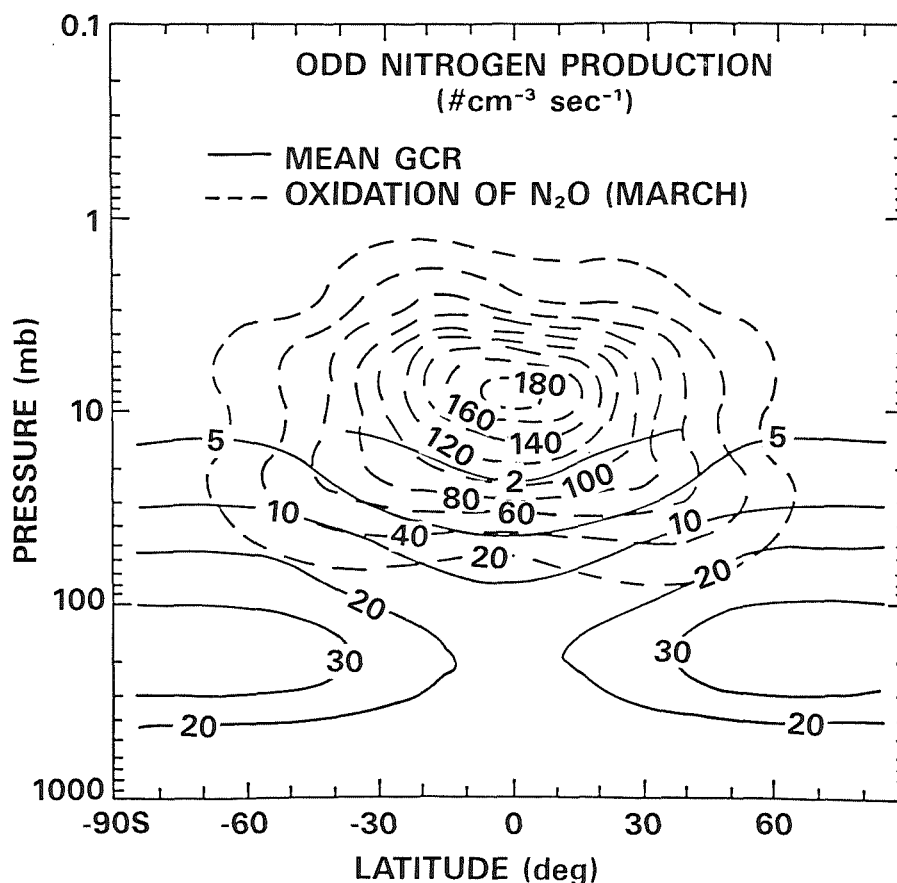


**Figure 9.** Odd nitrogen production (number  $cm^{-3} sec^{-1}$ ) caused by GCRs (solid line, from Figure 13 of Jackman et al. (36) and oxidation of nitrous oxide (dashed line, from Figure 9 of Jackman et al. (36).

Lightning is responsible for the production of significant amounts of odd nitrogen (of order  $3 \times 10^{35}$  molecules  $\text{yr}^{-1}$ ) from  $\text{N}_2$  in the free troposphere (35, 39-43). This source, along with others of tropospheric  $\text{NO}_y$ , can reach the stratosphere through the transport of tropospheric air across the tropopause. For example, the model source of lightning designated "H2" by Ko et al. (35) transports  $1.1 \times 10^{34}$  molecules of  $\text{NO}_y$   $\text{yr}^{-1}$  to the stratosphere when included in the NASA/Goddard 2-D model. Lower stratospheric background mixing ratios are increased substantially by including this lightning source. However, preliminary analysis of the STEP (Stratosphere Troposphere Exchange Project) data near the tropical tropopause show exceedingly low values of odd nitrogen ( $<0.5$  ppbv). The correlation of odd nitrogen with  $\text{N}_2\text{O}$  found on the aircraft missions to both the Antarctic (AAOE, Airborne Antarctic Ozone Experiment) and the Arctic (AASE, Airborne Arctic Stratospheric Expedition) is also consistent with the view that air entering the stratosphere contains low concentrations of odd nitrogen (44a,44b).

The production of odd nitrogen species by SPEs was predicted and shown to affect upper-stratospheric ozone (45). Since solar protons generally are at lower energies than GCRs, they produce NO at higher altitudes; they are constrained more significantly by the earth's magnetic field and affect the atmosphere only in the polar cap region (geomagnetic latitudes greater than about  $60^\circ$ ). SPEs are sporadic, with durations up to several days; more SPEs occur close to the solar maximum.

The increase in polar NO after the July 1982 SPE was inferred to be about  $6 \times 10^{14}$  NO molecules  $\text{cm}^{-2}$  ( $4.1 \times 10^{32}$  molecules  $\text{NO}_y$ ) at polar latitudes from the SBUV instrument (46), in good agreement with the calculated NO increase of  $7 \times 10^{14}$  NO molecules  $\text{cm}^{-2}$  ( $4.8 \times 10^{32}$  molecules  $\text{NO}_y$ ) in the polar cap (47). The August 1972 SPE was one of the biggest events in the past 30 years, and computations revealed that a substantial production of odd nitrogen ( $1.5 \times 10^{33}$  molecules  $\text{NO}_y$ ) was associated with this event at polar latitudes in the middle to upper stratosphere (47).

The influence of extreme ultraviolet, auroral electrons, and photoelectrons on the odd nitrogen budget of the stratosphere, through transport of odd nitrogen from the thermosphere downwards through the polar mesosphere to the upper stratosphere, has been studied by several groups (33,38,48-56). EUV, auroral electrons, and photoelectrons are capable of dissociating  $\text{N}_2$  to form atomic nitrogen in the thermosphere. Transport of this odd nitrogen to the mesosphere and upper stratosphere is possible, but certain conditions must be present. The lifetime of odd nitrogen in the sunlit mesosphere is short, and it is only during the long period of polar night at high latitudes, when a period of several weeks of darkness is typical, that significant downward transport is possible. Solomon et al. (51) undertook a detailed 2-D model study of thermosphere-middle atmosphere coupling. Enhancements in the odd nitrogen distribution in the mesosphere and upper stratosphere were found to occur when the thermospheric production of odd nitrogen was included [compare Figures 8 and 17 of Solomon et al. (51)]. These enhancements of  $\text{NO}_x$  in the middle atmosphere, caused by thermospheric downflux of odd nitrogen, are especially significant in the hemisphere that was most recently polar night. Measurements by the LIMS of  $\text{NO}_2$  have also indicated that odd nitrogen may be enhanced in the mesosphere and, to a lesser degree, in the upper stratosphere during polar night (55). The magnitude of the thermospheric downflux of  $\text{NO}_x$  into the stratosphere is highly uncertain and variable, but probably small.

In the past 15 years, it has been proposed that REPs make important contributions to the polar odd nitrogen budget of the mesosphere and upper stratosphere (57-62). The frequency and flux spectra of these REPs is still under discussion. Baker et al. (59) show evidence of large fluxes of relativistic electrons at geostationary orbit measured by the Spectrometer for Energetic Electrons (SEE) instrument on board spacecraft 1979-053 and 1982-019. REPs, which are actually depositing energy into the middle atmosphere, have been measured by

instruments aboard sounding rockets (63). These rocket measurements have typically indicated much smaller fluxes of relativistic electrons than measured by the SEE instrument. REPs that display the large fluxes measured by Baker et al. (59) are computed to show an important influence on the  $\text{NO}_y$  budget in the lower mesospheric-upper stratospheric region by Callis et al. (62). However, REPs with the smaller fluxes measured by Goldberg et al. (63) would cause a relatively insignificant change in odd nitrogen amounts in the middle atmosphere at this production rate. More work is necessary to determine which REP events are more typical. The global magnitude of the REP source of stratospheric odd nitrogen is also highly uncertain but probably small.

### Sources of Odd Nitrogen Related to Human Activity

The natural source of odd nitrogen is increasing because the source gas,  $\text{N}_2\text{O}$ , is increasing. The global rate of increase of  $\text{N}_2\text{O}$  is about  $0.7 \text{ ppbv yr}^{-1}$ ; the global average concentration is currently above 308 ppbv (16). At this rate of increase, assuming a linear increase in  $\text{N}_2\text{O}$  at all altitudes, the natural source of odd nitrogen will increase by 10% in 40 years. For comparison, the source of  $\text{NO}_y$  from stratospheric aircraft for with EI of 15 and  $7.7 \times 10^{10} \text{ kg of fuel yr}^{-1}$  is  $1.4 \times 10^{34}$  molecules  $\text{yr}^{-1}$ , nearly 40% of the natural source.

Atmospheric nuclear explosions, affecting the 7-to 30-km regime, cause sufficiently high temperatures in the fireball that thermal decomposition of  $\text{N}_2$  and  $\text{O}_2$  occurs, followed by the formation of NO (64-66). The nuclear tests in 1961 and 1962 by the Soviet Union and the United States were thought to be responsible for the production of  $2.4 \times 10^{34}$  molecules of odd nitrogen (16).

### Sinks of Odd Nitrogen

There are two major sinks for odd nitrogen in the stratosphere: the recombination of N and NO in the middle to upper stratosphere, to form  $\text{N}_2$  and O, and transport to the troposphere. Nitric oxide (NO) is photodissociated easily in the upper stratosphere, forming atomic nitrogen (N) and atomic oxygen (O). Some of this N then reacts with NO, to form molecular nitrogen ( $\text{N}_2$ ); the rest reacts with  $\text{O}_2$  to reform NO. The lower stratospheric odd nitrogen abundance is principally regulated by transport of odd nitrogen to the troposphere, with subsequent rainout of the  $\text{HNO}_3$  and  $\text{HO}_2\text{NO}_2$  constituents [see Jackman et al. (36)].

The global annually averaged loss for the first process is about  $8.4 \times 10^{33}$  molecules  $\text{yr}^{-1}$  (Jackman and Douglass, 2-D model computation, 1990). The remainder of the globally averaged production is balanced by the transport of stratospheric odd nitrogen to the troposphere ( $4.0 \times 10^{34} - 0.8 \times 10^{34} = 3.2 \times 10^{34}$ ), the dominant loss mechanism for stratospheric odd nitrogen. Thus the amount of odd nitrogen in the lower stratosphere depends critically on the circulation in the lower stratosphere and stratosphere/troposphere exchange.

### Odd Nitrogen Distribution

The global distribution of total odd nitrogen may be calculated using a 2-D model, keeping in mind that the model transport in the upper troposphere/lower stratosphere is important to determining distribution and residence time of total odd nitrogen. Although there are no global measurements of total odd nitrogen, Callis et al. (67) estimate total odd nitrogen from nighttime LIMS measurements of  $\text{NO}_2$  and  $\text{HNO}_3$ . Using a model, they show that this sum represents 68, 78, 85, and 90% of total odd nitrogen at, respectively, 28, 34, 37, and 40 km. The estimate from LIMS for March (Figure 10) can be compared to the calculations of the Jackman and Douglass model (Figure 11), or to several model distributions given by Jackman et al. (7). Although the data represent a lower limit because all species are not included, notably



$N_2O_5$ , the model values are somewhat lower than the measurements in the lower stratosphere. It should be noted that the lower stratospheric LIMS values of  $NO_2$  depend on the  $NO_2$  climatology used in the retrievals resulting from a loss of  $NO_2$  signal from altitudes below 40 mb (68). Thus the LIMS data can provide constraints on the odd nitrogen species but do not provide a direct measure of  $NO_y$ .

In situ measurements of total odd nitrogen taken aboard the NASA ER-2 aircraft provide several points for direct comparison between models and data. The ambient total odd nitrogen is measured by catalytic conversion of the higher-oxide species to  $NO$  and subsequent detection of  $NO$  in the chemiluminescent reaction with reagent  $O_3$ . All odd nitrogen species of importance in the stratosphere are included in this technique (69). Although measured odd nitrogen in the lower stratosphere and upper troposphere has substantial natural variability on a wide range of scales, the data are sufficient to derive representative averages at some locations and seasons. Extensive measurements in the winter hemispheres near  $55^\circ S$  and  $60^\circ N$  show odd nitrogen values less than 0.5 ppbv in the troposphere, up to about 10 km altitude, increasing to about 3 ppbv near 16 km and to about 8 ppbv near 20 km (70,71). Values of 3 to 8 ppbv between 19 and 21 km were measured near  $40^\circ N$  in October (72). Measurements near  $10^\circ S$  in January and February gave tropospheric odd nitrogen values similar to those measured at high latitudes but significantly lower values in the lower stratosphere. Odd nitrogen values near  $10^\circ S$  increase from about 0.5 ppbv near the tropopause to about 2.5 ppbv near 21 km (73). The model values in Figure 11 underestimate the measured total odd nitrogen. Previous ER-2  $NO$  measurements have suggested this discrepancy (4,74). The ATMOS (Atmospheric Trace Molecule Spectroscopy) measurements of total odd nitrogen are as much as 40% larger than the results from some model calculations for the lower stratosphere (75).

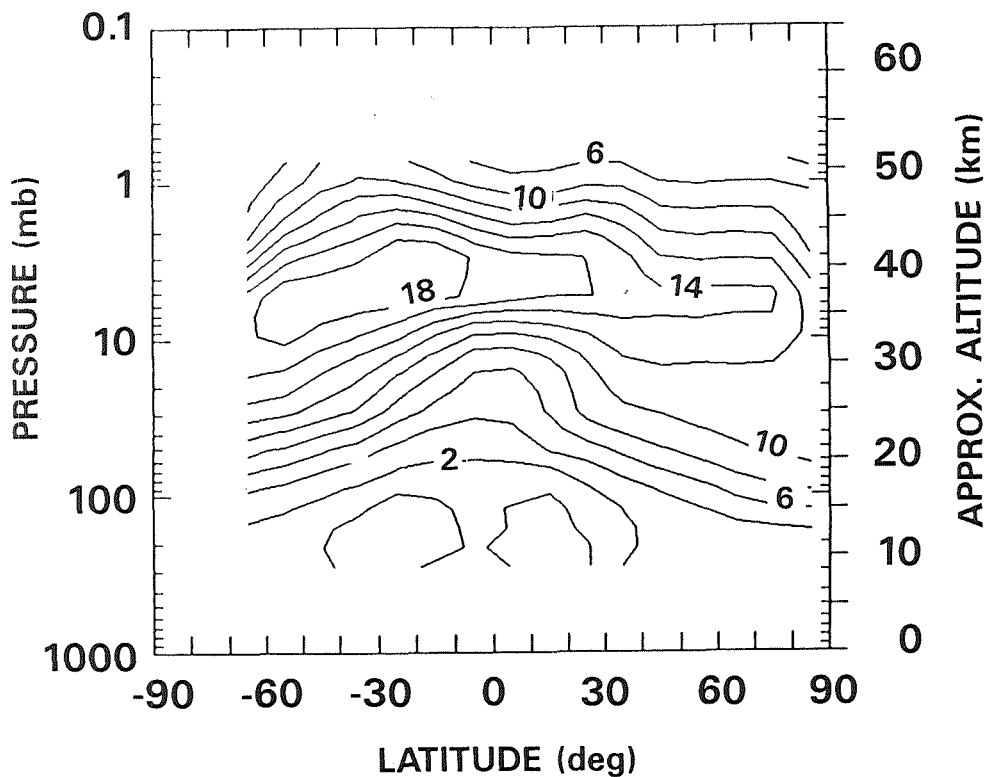


Figure 10. LIMS nighttime  $HNO_3 + NO_2$  for March 1979, a lower limit for total  $NO_y$ .

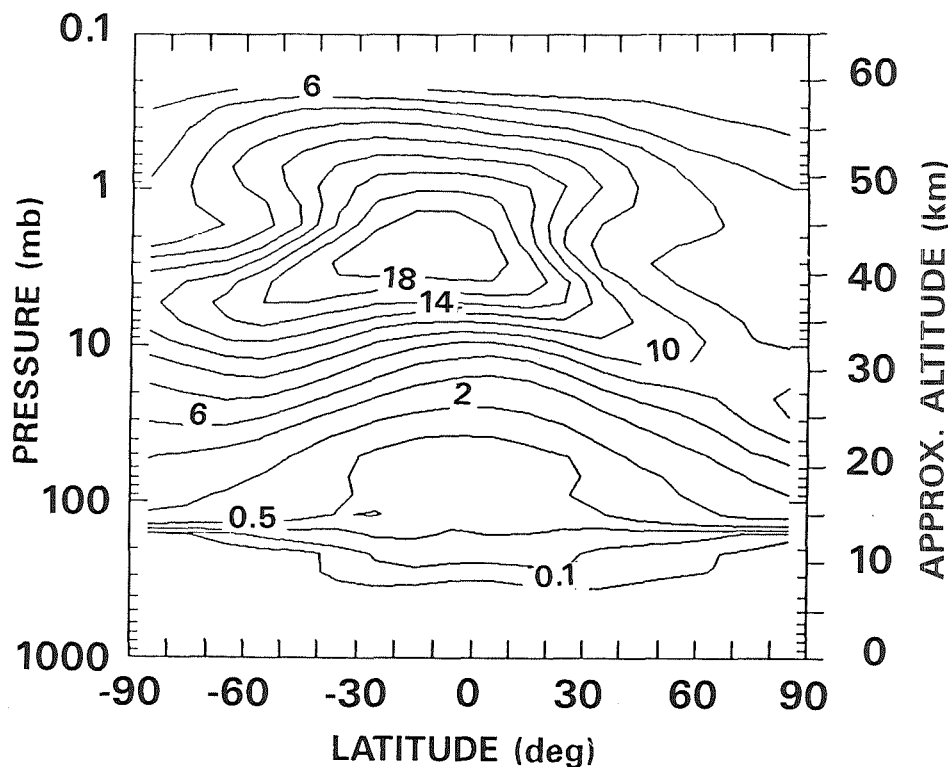


Figure 11. A 2-D model calculation of total odd nitrogen (March).

### Partitioning of Odd Nitrogen Species

The lifetimes for interchange reactions among key odd nitrogen species, calculated from the NASA/Goddard 2-D model, are given for March equinox in Figure 12. Once  $\text{HNO}_3$  is formed in the lower stratosphere, it is relatively long lived ( $> 50$  days for middle and high latitudes). The lifetime of  $\text{N}_2\text{O}_5$  is short, except in high latitudes in winter. The equilibrium between  $\text{NO}$  and  $\text{NO}_2$  is established quickly; thus, the fractions of  $\text{NO}$  and  $\text{NO}_2$  in the aircraft exhaust are not important for assessment calculations. Some studies have likewise shown an insensitivity to the relative partitioning between  $\text{NO}_x$  and  $\text{HNO}_3$  in stratospheric injections, but this is not likely to be the case for tropospheric emissions.

However, the current understanding of odd nitrogen chemistry in the lower stratosphere does not explain all of the observations. For example, measured values of wintertime  $\text{HNO}_3$  exceed model calculated values (35). Some investigators have suggested that the heterogeneous reaction of  $\text{N}_2\text{O}_5$  on polar stratospheric clouds (PSCs) in the polar vortex may produce the observed values (76). Rood et al. (77) have found, with 3-D model calculations, that there is insufficient mixing between the polar vortex and middle latitudes to account for the  $\text{HNO}_3$  deficit. Measurements of reaction rates show that  $\text{N}_2\text{O}_5 + \text{H}_2\text{O}$  reactions occur on sulfuric acid, even though some of the other processes that occur on PSC surfaces (e.g.,  $\text{HCl} + \text{ClONO}_2$ ) do not (18). Hofmann and Solomon (78) suggested that such heterogeneous reactions on background aerosols could account for the observations. These processes are important for understanding the natural balance of  $\text{HNO}_3$  and  $\text{NO}_x$ . The potential impact of aircraft exhaust on stratospheric ozone is sensitive to this balance.

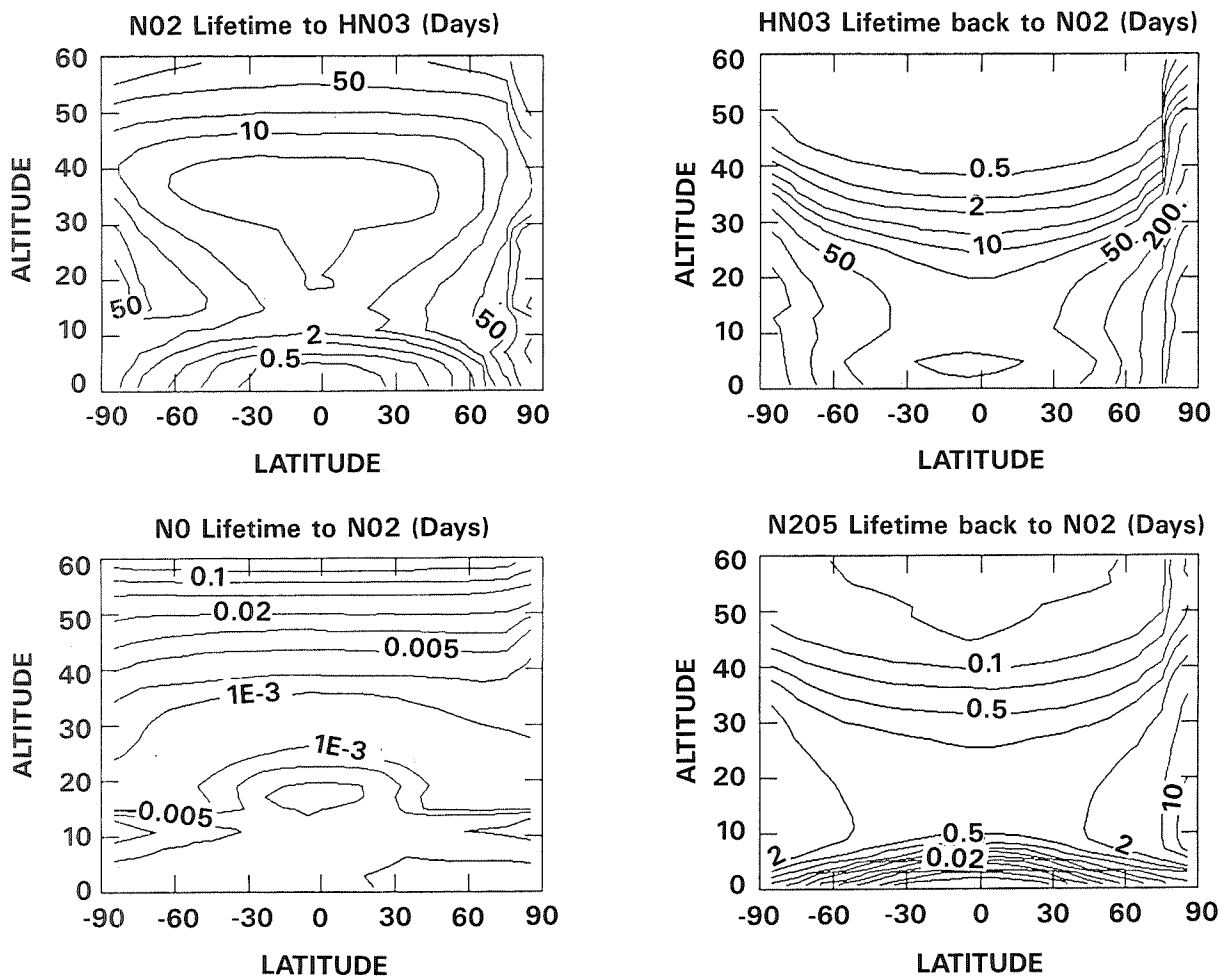


Figure 12. Lifetimes for interconversions among odd nitrogen species (March).

## HYDROCARBONS

The lower troposphere contains a wide variety of hydrocarbons. Most of these are destroyed by reactions with the hydroxyl radical. Only those species with photochemical lifetimes longer than a few months reach the tropical tropopause in sufficient concentration to affect stratospheric chemistry. This restricts the population to methane (CH<sub>4</sub>) and the nonmethane hydrocarbons (NMHC) acetylene (C<sub>2</sub>H<sub>2</sub>), ethane (C<sub>2</sub>H<sub>6</sub>), and propane (C<sub>3</sub>H<sub>8</sub>).

The methane distribution is fairly well established on several spatial scales. Data from the period 1983-87, from the surface and mid-troposphere, indicate that CH<sub>4</sub> is increasing by about 1% per year (16). During the 1980s, the average free tropospheric mixing ratio in the northern hemisphere was about 1.7 ppm, while in the southern hemisphere it was somewhat less, 1.6 ppm. The stratospheric distribution has been determined by several groups measuring primarily at midlatitudes and using balloon-borne instruments. The SAMS measurements pro-

vide a global picture of the behavior of  $\text{CH}_4$  above 20 mb. The maximum stratospheric mixing ratio is seen in the tropical lower stratosphere; the mixing ratio decreases poleward and with altitude. A detailed description of the data and comparison with model calculations are given by Jones and Pyle (79).

Nonmethane hydrocarbons have considerable seasonal and spatial variation in the troposphere and we may expect similarly large variations in the lower stratosphere as well. Average lifetimes for  $\text{C}_3\text{H}_8$ ,  $\text{C}_2\text{H}_2$ , and  $\text{C}_2\text{H}_6$  are 0.06 yr, 0.1 yr, and 0.25 yr, respectively, but vary according to locale and may be much shorter in the tropics. Based on limited observations, we may describe the distribution of NMHCs as follows. The NMHCs increase from the South Pole towards the equator, (80-84), peaking at northern midlatitudes. Typical tropospheric northern midlatitude values for the NMHCs are 0.2 ppb acetylene, 2 ppb ethane, and 0.6 ppb propane. The seasonal cycle is dominated by variations in OH. In the Arctic, ethane has a maximum mixing ratio in the winter; and is 2 times less in summer. The annual variation of propane is greater (85). In Antarctica (86), ethane has a winter value of 0.45 ppb, with a summer mixing ratio of 0.3 ppb. The corresponding figures for acetylene are 20 and 10 ppt, respectively, and the propane content varies from 0.05 to 0.1. ppb.

Vertical distributions of the NMHCs in the stratosphere have only been measured at northern midlatitudes. With the exception of a limited number of satellite measurements, information has been by balloon-borne samplers (83,87-90) or by analysis of solar absorption spectra taken from the ground or aircraft (91-93). The vertical profile of ethane is nearly constant to 10-km altitude, with a mixing ratio between 1.5 and 2 ppb. The mixing ratio drops by an order of magnitude at 15 km and by 2 orders of magnitude at 25 km. This vertical distribution is confirmed by analysis of spectra profiles of solar infrared radiation (94). The measured vertical profiles of propane are confined to altitudes below 20 km. At 10 km, mixing ratios are between 0.2 and 0.8 ppb; at 17 km, the mixing ratio is 0.1 ppb. Acetylene, as measured at 10 km by direct sampling, has a value between 0.1 and 0.23 ppb. By 16 km, the mixing ratio is 0.02 ppb. The vertical distribution of molecules like ethane could be important in the chemistry of the stratosphere by serving as a tracer for the OH and Cl radical profiles (95). The breakdown of the NMHCs can modify the photochemistry of the lower stratosphere and upper troposphere (96-99).

The lifetimes of NMHCs can be significantly shorter in the stratosphere than in the troposphere as a result of reactions with Cl and are often less than 1 month. If this estimate of the lifetime is correct, the magnitude of the increase in the concentrations of the hydrocarbons in aircraft exhaust is controlled by photochemical loss rather than transport. Pollutant molecules are destroyed by reactions with OH and Cl, the perturbation is limited directly by the amount of pollutant in the aircraft exhaust. An important role of  $\text{CH}_4$  and NMHCs in the lower stratosphere is to convert Cl to HCl and to produce ozone by reactions of NO with oxidation products, e.g.,  $\text{HO}_2$  and  $\text{CH}_3\text{O}_2$ . The rate of oxidation of background  $\text{CH}_4$  in the lower stratosphere ( $1-5 \times 10^{10}$  molecules  $\text{cm}^{-3} \text{s}^{-1}$ ) is much larger than the source of hydrocarbons in the aircraft exhaust (about  $1 \times 10^8$  molecules  $\text{cm}^{-3} \text{s}^{-1}$  if mixed in the northern hemisphere over an altitude thickness of 5 km). The picture could be somewhat more complicated by addition of reactions to form nitrates such as peroxy acetyl nitrate (PAN) in the high  $\text{NO}_x$  environment of the aircraft plume. However, although PAN is somewhat longer lived than the hydrocarbons, the summer lifetime is less than 3 months, and the maximum perturbation is still controlled by photochemistry.

## CONCLUSION

The species considered here, most obviously the odd nitrogen species, influence the photochemical balance of the lower stratosphere. Perturbations to these species may have a direct impact on the ozone concentration in the lower stratosphere, even though time scales for photochemical processes such as ozone destruction are in the range of several years. For the species that are long lived in the lower stratosphere, the magnitudes of the possible perturbations to the background values of the components of stratospheric aircraft exhaust are controlled by the mass flow through the region in which the aircraft exhaust is mixed. This underscores the importance of understanding stratosphere/troposphere exchange and the circulation in the lower stratosphere where, it has been proposed, the high-speed civil transport will fly.

## REFERENCES

1. Brewer, A.W., Evidence for a world circulation provided by the measurements of helium and water vapor distribution in the stratosphere, *Quart. J. Roy. Met. Soc.*, 75, 351-363, 1949.
2. Dobson, G.M.B., Origin and distribution of the polyatomic molecules in the atmosphere, *Proc. Roy. Soc. London Ser. A*, 236, 187-193, 1956.
3. Mahlman, J.D., Mechanistic Interpretation of Stratospheric Tracer Transport, in *Advances in Geophysics, Vol. 28, Issues in Atmospheric and Oceanic Modeling*, edited by Syukuro Manabe, Academic Press, Inc., 301-326, 1985.
4. World Meteorological Organization, Atmospheric ozone 1985: Assessment of our understanding of the processes controlling its present distribution and change, *Global Ozone Res. and Monitoring Proj. Rep. 16*, Geneva, 1986.
5. Dunkerton, T.J., On the mean meridional mass motions of the stratosphere and mesosphere, *J. Atmos. Sci.*, 35, 2325-2333, 1978.
6. Rood, R.B., and M.R. Schoeberl, A mechanistic model of Eulerian, Lagrangian mean, and Lagrangian ozone transport by steady planetary waves, *J. Geophys. Res.*, 88, 5208, 5218, 1983.
7. Jackman, C.H., R.K. Seals, Jr., and M.J. Prather, Two-Dimensional Intercomparison of Stratospheric Models, NASA Conference Publication 3042, 1989.
8. Andrews, D.G., J.R. Holton, and C.B. Leovy, *Middle Atmosphere Dynamics*, Academic Press, Inc., 1987.
9. Jackman, C.H., A.R. Douglass, P.D. Guthrie, and R.S. Stolarski, The sensitivity of total ozone and ozone perturbation scenarios in a two-dimensional model due to dynamical inputs, *J. Geophys. Res.*, 97, 9873-9887, 1989.
10. Douglass, A.R., C.H. Jackman, and R.S. Stolarski, Comparison of model results transporting the odd nitrogen family with results transporting separate odd nitrogen species, *J. Geophys. Res.*, 94, 9862-9872, 1989.
11. Shia, R.L., Y.L. Unig, M. Allen, R.W. Zurek, and D. Crisp, Sensitivity study of advection and diffusion coefficients in a two-dimensional stratospheric model using excess carbon 14 data, *J. Geophys. Res.*, 94, 18,467-18,484, 1989.
12. Holton, J.R., On the global exchange of mass between the stratosphere and troposphere, *J. Atmos. Sci.*, 47, 392-395, 1990.
13. Robinson, G.D., The transport of minor atmospheric constituents between troposphere and stratosphere, *Quart. J. Roy. Meteor. Soc.*, 106, 227-253, 1980.
14. Volz, A., U. Schmidt, J. Rudolph, D.H. Ehhalt, F.J. Johnson, and A. Khedim, "Vertical Profiles of Trace Gases as Mid-Latitudes," Jul-Report No. 1742, Kernforschungsanlage, Julich, Federal Republic of Germany, 1981.

15. Gamo, T., M. Tsutsumi, H. Sakai, T. Nakazawa, M. Tanaka, H. Honda, H. Kubo, and T. Itoh, Carbon and oxygen isotopic ratios of carbon dioxide of a stratospheric profile over Japan, *Tellus*, 41b, 127-133, 1989.
16. World Meteorological Organization, Report of the International Ozone Trends Panel 1988, *Global Ozone Research and Monitoring Project - Report No. 18*, Geneva, 1990.
17. Jackman, C.H., R.S. Stolarski, and J.A. Kaye, Two-dimensional monthly average ozone balance from limb infrared monitor of the stratosphere and stratospheric and mesospheric sounder data, *J. Geophys. Res.*, 91, 1103-1116, 1986.
18. Tolbert, M.A., M.J. Rossi, and D.M. Golden, Heterogeneous interactions of ClONO<sub>2</sub>, HCl and HNO<sub>3</sub> with sulfuric acid surfaces at stratospheric temperatures, *Geophys. Res. Lett.*, 15, 851-854, 1988.
19. Worsnop, D., M. Zahniser, C. Kolb, L. Watson, J. Van Doren, J. Jayne, and P. Davidovits, Mass accommodation coefficient measurements for HNO<sub>3</sub>, HCl, and N<sub>2</sub>O<sub>5</sub> on water, ice, and aqueous sulfuric acid droplet surfaces, paper presented at the Polar Ozone Workshop, NASA/NOAA/NSF/CMA, Snowmass, CO May 9-13, 1988.
20. Mozurkewich, M., and J.G. Calvert, Reaction probability of N<sub>2</sub>O<sub>5</sub> on aqueous aerosols, *J. Geophys. Res.*, 93, 15,889-15,896, 1988.
21. LeTexier, H., S. Solomon, and R.R. Garcia, The role of molecular hydrogen and methane oxidation in the water vapor budget of the stratosphere, *Quart. J. Roy. Meteor. Soc.*, 114, 281-295, 1988.
22. Kley, D., A.L. Schmeltekopf, K. Kelley, R.H. Winkler, T.L. Thompson, and M. McFarland, Transport of water vapor through the tropical tropopause, *Geophys. Res. Lett.*, 9, 617-620, 1982.
23. Mastenbrook, H.J., and S.J. Oltmans, Stratospheric water variability for Washington, DC/Boulder, CO: 1964-82, *J. Atmos. Sci.*, 40, 2157-2165, 1983.
24. Russell, J.M., III, J.C. Gille, E.M. Remsberg, L.L. Gordley, P.L. Bailey, H. Fischer, A. Girard, S.R. Drayson, W.F.J. Evans, and J.E. Harries, Validation of water vapor results measured by the Limb Infrared Monitor of the Stratosphere experiment on NIMBUS 7, *J. Geophys. Res.*, 89, 5115-5124, 1984.
25. Rind, D., E-W. Chiou, W.P. Chu, S. Oltmans, J. Lerner, J.C. Larsen, M.P. McCormick, and L.R. McMaster, Positive water vapor feedback in climate models confirmed by satellite data, *Nature*, 349, 500-503, 1991.
26. Rind, D., E-W. Chiou, W. Chu, S. Oltmans, J. Lerner, J. Larsen, M.P. McCormick, and L. McMaster, Overview of the SAGE II water vapor observations: method, validation and data characteristics, submitted to *J. Geophys. Res.*, 1991.
27. Chiou, E-W., M.P. McCormick, L. McMaster, W.P. Chu, J.C. Larsen, D. Rind, and S. Oltmans, Intercomparison of stratospheric water vapor observed by satellite experiments, submitted to *J. Geophys. Res.*, 1991.

28. Chu, W., E-W. Chiou, J.C. Larsen, L. Thomason, D. Rind, J.J. Buglia, M.P. McCormick, and L.R. McMaster, Algorithms and error estimates for SAGE II water vapor retrievals. submitted to *J. Geophys. Res.*, 1991.
29. Larsen, J.C., D. Rind, S. Oltmans, E-W. Chiou, W.P. Chu, M.P. McCormick, and L.R. McMaster, Comparison of the SAGE II Tropospheric water vapor to radiosonde measurements, submitted to *J. Geophys. Res.*, 1991.
30. McCormick, M.P., E-W. Chiou, L.R. McMaster, W.P. Chu, J.C. Larsen, D. Rind, and S. Oltmans, Seasonal variations of water vapor, submitted to *J. Geophys. Res.*, 1991.
31. Oltmans, S., W. Chu, E. Chiou, L.R. McMaster, M.P. McCormick, D. Rind, and J. Larsen, submitted to *J. Geophys. Res.*, 1991.
32. Johnston, H.S., O. Serang, and J. Podolski, Instantaneous global nitrous oxide photochemical rates, *J. Geophys. Res.*, *84*, 5077-5082, 1979.
33. Jackman, C.H., J.E. Frederick, and R.S. Stolarski, Production of odd nitrogen in the stratosphere and mesosphere: An intercomparison of source strengths, *J. Geophys. Res.*, *85*, 7495-7505, 1980.
34. Crutzen, P.J., and U. Schmailzl, Chemical budgets of the stratosphere, *Planet. Space Sci.*, *31*, 1009-1032, 1983.
35. Ko, M.K.W., M.B. McElroy, D.K. Weisenstein, and N.D. Sze, Lightning: A possible source of stratospheric odd nitrogen, *J. Geophys. Res.*, *91*, 5395-5404, 1986.
36. Jackman, C.H., P.D. Guthrie, and J.A. Kaye, An intercomparison of nitrogen-containing species in Nimbus 7 LIMS and SAMS data, *J. Geophys. Res.*, *92*, 995-1008, 1987.
37. Nicolet, M., On the production of nitric oxide by cosmic rays in the mesosphere and stratosphere, *Planet. Space Sci.*, *23*, 637-649, 1975.
38. Legrand, M.R., F. Stordal, I.S.A. Isaksen, and B. Rognerud, A model study of the stratospheric budget of odd nitrogen, including effects of solar cycle variations, *Tellus*, *41B*, 413-426, 1989.
39. Noxon, J.F., Atmospheric nitrogen fixation by lightning, *Geophys. Res. Lett.*, *3*, 463-465, 1976.
40. Tuck, A.F., Production of nitrogen oxides by lightning discharges, *Quart. J. Roy. Met. Soc.*, *102*, 749-755, 1976.
41. Chameides, W.L., D.H. Stedman, R.R. Dickerson, D.W. Rusch, and R.J. Cicerone, NO<sub>x</sub> production in lightning, *J. Atmos. Sci.*, *34*, 143-149, 1977.
42. Logan, J.A., Nitrogen oxides in the troposphere: Global and regional budgets, *J. Geophys. Res.*, *88*, 10,785-10,807, 1983.
43. Borucki, W.J., and W.L. Chameides, Lightning: Estimates of the rates of energy dissipation and nitrogen fixation, *Rev. Geophys.*, *22*, 363-372, 1984.



- 44a. Fahey, D.W., K.K. Kelly, S.R. Kawa, A.F. Tuck, M. Loewenstein, K.R. Chan, and L.E. Heidt, Observations of denitrification and dehydration in the winter polar stratospheres, *Nature*, 344, 321-324, 1990.
- 44b. Fahey, D.W., S. Solomon, S.R. Kawa, M. Loewenstein, J.R. Podolske, S.E. Strahan, and K.R. Chan, A diagnostic for denitrification in the winter polar stratospheres, *Nature*, 345, 698-702, 1990.
45. Crutzen, P.J., I.S.A. Isaksen, and G.C. Reid, Solar proton events: Stratospheric sources of nitric oxide, *Science*, 189, 457-458, 1975.
46. McPeters, R.D., A nitric oxide increase observed following the July 1982 solar proton event, *Geophys. Res. Lett.*, 13, 667-670, 1986.
47. Jackman, C.H., A.R. Douglass, R.B. Rood, R.D. McPeters, and P.E. Meade, Effect of solar proton events on the middle atmosphere during the past two solar cycles as computed using a two-dimensional model, *J. Geophys. Res.*, 95, 7417-7428, 1990.
48. Strobel, D.F., Odd nitrogen in the mesosphere, *J. Geophys. Res.*, 76, 8384-8393, 1971.
49. McConnell, J.C., and M.B. McElroy, Odd nitrogen in the atmosphere, *J. Atmos. Sci.*, 30, 1465-1480, 1973.
50. Brasseur, G., and M. Nicolet, Chemospheric processes of nitric oxide in the mesosphere and stratosphere, *Planet. Space Sci.*, 21, 939-961, 1973.
51. Solomon, S., P.J. Crutzen, and R.G. Roble, Photochemical coupling between the thermosphere and the lower atmosphere, 1, Odd nitrogen from 50 to 120 km, *J. Geophys. Res.*, 87, 7206-7220, 1982.
52. Frederick, J.E., and N. Orsini, The distribution and variability of mesospheric odd nitrogen: A theoretical investigation, *J. Atmos. Terr. Phys.*, 44, 479-488, 1982.
53. Garcia, R.R., S. Solomon, R.G. Roble, and D.W. Rusch, A numerical response of the middle atmosphere to the 11-year solar cycle, *Planet Space Sci.*, 32, 411-423, 1984.
54. Solomon, S., and R.R. Garcia, Transport of thermospheric NO to the upper stratosphere?, *Planet. Space Sci.*, 32, 399-409, 1984.
55. Russell, J.M., III, S. Solomon, L.L. Gordley, E.E. Remsberg, and L.B. Callis, The variability of stratospheric and mesospheric NO<sub>2</sub> in the polar winter night observed by LIMS, *J. Geophys. Res.*, 89, 7267-7275, 1984.
56. Brasseur, G., Coupling between the thermosphere and the stratosphere: The role of nitric oxide, *MAP Handbook*, Volume 10, 1984.
57. Thorne, R.M., Energetic radiation belt electron precipitation: A natural depletion mechanism for stratospheric ozone, *Science*, 195, 287-289, 1977.
58. Thorne, R.M., The importance of energetic particle precipitation on the chemical composition of the middle atmosphere, *Pure Appl. Geophys.*, 118, 128-151, 1980.

59. Baker, D.N., J.B. Blake, D.J. Gorney, P.R. Higbie, R.W. Klebesadel, and J.H. King, Highly relativistic magnetospheric electrons: A role in coupling to the middle atmosphere?, *Geophys. Res. Lett.*, 14, 1027-1030, 1987.
60. Sheldon, W.R., J.R. Benbrook, and E.A. Bering III, Comment on "Highly relativistic magnetospheric electrons: A role in coupling to the middle atmosphere?," *Geophys. Res. Lett.*, 15, 1449-1450, 1988.
61. Baker, D.N., J.B. Blake, D.J. Gorney, P.R. Higbie, R.W. Klebesadel, and J.H. King, Reply, *Geophys. Res. Lett.*, 15, 1451-1452, 1988.
62. Callis, L.B., D.N. Baker, J.B. Blake, J.D. Lambeth, R.E. Boughner, M. Natarajan, R.W. Klebesadel, and D.J. Gorney, Precipitating relativistic electrons: their long-term effect on stratospheric odd nitrogen levels, *J. Geophys. Res.*, 96, 2939-2976, 1991.
63. Goldberg, R.A., C.H. Jackman, J.R. Barcus, and F. Soraas, *J. Geophys. Res.*, 89, 5581-5596, 1984.
64. Johnston, H., G. Whitten, and J. Birks, Effect of nuclear explosions on stratospheric nitric oxide and ozone, *J. Geophys. Res.*, 78, 6107-6135, 1973.
65. Foley, H.M., and Ruderman, M.A., Stratospheric NO production from past nuclear explosions, *J. Geophys. Res.*, 78, 4441-4450, 1973.
66. Gilmore, F.R., The production of nitrogen oxides by low-altitude nuclear explosions, *J. Geophys. Res.*, 80, 4553-4554, 1975.
67. Callis, L.B., M. Natarajan, and J.M. Russell III, Estimates of the stratospheric distribution of odd nitrogen from the LIMS data, *Geophys. Res. Lett.*, 12, 259-262, 1985.
68. Remsberg, E.E., and J.M. Russell III, The Near Global Distributions of Middle Atmospheric H<sub>2</sub>O and NO<sub>2</sub> Measured by the Nimbus 7 LIMS Experiment, in *Transport Processes in the Middle Atmosphere*, edited by G. Visconti and R. Garcia, D. Reiden Publishing Company, 87-102, 1987.
69. Fahey, D.W., C.S. Eubank, G. Hubler, and F.C. Fehsenfeld, Evaluation of a catalytic reduction technique for the measurement of total reactive odd nitrogen NO<sub>y</sub> in the atmosphere, *J. Atmos. Chem.*, 3, 435-468, 1985.
70. Fahey, D.W., D.M. Murphy, K.K. Kelly, M.K.W. Ko, M.H. Proffitt, C.S. Eubank, G.V. Ferry, M. Loewenstein, and K.R. Chan, Measurements of nitric oxide and total reactive nitrogen in the Antarctic stratosphere: observations and chemical implications, *J. Geophys. Res.*, 94, 16,665-16,681, 1989.
71. Kawa, S.R., D.W. Fahey, L.C. Anderson, M. Loewenstein, and K.R. Chan, Measurements of total reactive nitrogen during the Airborne Arctic Stratospheric Expedition, *Geophys. Res. Lett.*, 17, 485-488, 1990.
72. Kawa, S.R., D.W. Fahey, S. Solomon, W.H. Brune, M.H. Proffitt, D.W. Toohey, D.E. Anderson, Jr., L.C. Anderson, and K.R. Chan, Interpretation of aircraft measurements of NO, ClO, and O<sub>3</sub> in the lower stratosphere, *J. Geophys. Res.*, 95, 18,597-18,609, 1990.

73. Fahey, D.W., Unpublished data, 1991.
74. Loewenstein, M., W.J. Borucki, H.F. Savage, J.G. Borucki, and R.C. Whitten, Geographical variations of NO and O<sub>3</sub> in the lower stratosphere, *J. Geophys. Res.*, **83**, 1875-1882, 1978.
75. Russell, J.M., III, C.B. Farmer, C.T. Rinsland, R. Zander, L. Froidevaux, G.C. Toon, B. Gao, J. Shaw, and M. Gurnson, Measurements of Odd Nitrogen Compounds in the Stratosphere by the ATMOS Experiment on Space Lab 3, *J. Geophys. Res.*, **93**, 1718-1736, 1988.
76. Austin, J., R.R. Garcia, J.M. Russell III, S. Solomon, and A.F. Tuck, On the atmospheric photochemistry of nitric acid, *J. Geophys. Res.*, **91**, 5477-5485, 1986.
77. Rood, R.B., J.A. Kaye, A.R. Douglass, D.J. Allen, S. Steenrod, and E.M. Larson, Wintertime nitric acid chemistry: implications from three-dimensional model calculations, *J. Atmos. Sci.*, **47**, 2696-2709, 1990.
78. Hofmann, D.J., and S. Solomon, Ozone destruction through heterogeneous chemistry following the eruption of El Chichon, *J. Geophys. Res.*, **94**, 5029-5042, 1989.
79. Jones, R.L., and J.A. Pyle, Observations of CH<sub>4</sub> and N<sub>2</sub>O by the NIMBUS 7 SAMS: A comparison with in situ data and two-dimensional numerical model calculations, *J. Geophys. Res.*, **89**, 5263-5279, 1984.
80. Rudolph, J., and D.H. Ehhalt, Measurements of C<sub>2</sub>-C<sub>5</sub> hydrocarbons over the North Atlantic, *J. Geophys. Res.*, **86**, 11959-11964, 1981.
81. Singh, H.B., and L.J. Salas, Measurement of selected light hydrocarbons over the Pacific Ocean: latitudinal and seasonal variations, *Geophys. Res. Lett.*, **9**, 842-845, 1982.
82. Blake, D.R., and F.S. Rowland, Global atmospheric concentrations and source strength of ethane, *Nature*, **321**, 231-233, 1986.
83. Ehhalt, D.H., J. Rudolph, F. Meixner, and U. Schmidt, Measurements of selected C<sub>2</sub>-C<sub>5</sub> hydrocarbons in the background troposphere: vertical and latitudinal variations, *J. Atm. Chem.*, **3**, 29-52, 1985.
84. Singh, H.B., W. Viezee, and Louis J. Salas, Measurements of selected C<sub>2</sub>-C<sub>5</sub> hydrocarbons in the troposphere: latitudinal, vertical and temporal variations, *J. Geophys. Res.*, **93**, 15861-15878, 1988.
85. Tille, K.J.W., M. Savelsberg, and K. Bachmann, Airborne measurements of nonmethane hydrocarbons over western europe: vertical distributions, seasonal cycles of mixing ratios and source strengths, *Atmos. Environ.*, **19**, 1751-1760, 1985.
86. Rudolph, J., A. Khedim, and D. Wagenbach, The seasonal variation of light nonmethane hydrocarbons in the Antarctic troposphere, *J. Geophys. Res.*, **94**, 13,039-13,044, 1989.
87. Robinson, E., Hydrocarbons in the atmosphere, *Pure Appl. Geophys.*, **116**, 372-384, 1978.

88. Cronn, D., and E. Robinson, Tropospheric and lower stratospheric vertical profiles of ethane and acetylene, *Geophys. Res. Lett.*, 6, 641-644, 1979.
89. Rudolph, J., D.H. Ehhalt, and A. Tonnissen, Vertical profiles of ethane and propane in the stratosphere, *J. Geophys. Res.*, 86, 7267-7272, 1981.
90. Aikin, A.C., C.C. Gallagher, W.C. Spicer, and M.W. Holdren, Measurement of methane and other light hydrocarbons in the troposphere and lower stratosphere, *J. Geophys. Res.*, 92, 3135-3138, 1987.
91. Goldman, A., F.J. Murcray, R.D. Blatherwick, J.R. Gillis, F.S. Bonomo, F.H. Murcray, and D.G. Murcray, Identification of acetylene ( $C_2H_2$ ) in infrared atmospheric absorption spectra, *J. Geophys. Res.*, 86, 12143-12146, 1981.
92. Goldman, A., C.P. Rinsland, F.J. Murcray, D.G. Murcray, M.T. Coffey, and W.G. Mankin, Balloon-borne and aircraft infrared measurements of ethane ( $C_2H_6$ ) in the upper troposphere and lower stratosphere, *J. Atmos. Chem.*, 2, 211-221., 1984.
93. Coffey, M.T., W.G. Mankin, A. Goldman, C.P. Rinsland, G.A. Harvey, V. Malathy Devi, and G.M. Stokes, Infrared measurements of atmospheric ethane ( $C_2H_6$ ) from aircraft and ground based solar absorption spectra in the  $3000\text{ cm}^{-1}$  region, *Geophys. Res. Lett.*, 12, 199-202, 1985.
94. Rinsland, C.P., R. Zander, C.B. Farmer, R.H. Norton, and J.M. Russell III, Concentrations of ethane ( $C_2H_6$ ) in the lower stratosphere and upper troposphere and acetylene ( $C_2H_2$ ) in the upper troposphere deduced from atmospheric trace molecule spectroscopy/spacelab 3 spectra, *J. Geophys. Res.*, 92, 11951-11964, 1987.
95. Chameides, W.L., and R.J. Cicerone, Effects of nonmethane hydrocarbons in the atmosphere, *J. Geophys. Res.*, 83, 947-952, 1978.
96. Aikin, A.C., J.R. Herman, E.J. Maier, and C.J. McQuillan, Atmospheric chemistry of ethane and ethylene, *J. Geophys. Res.*, 87, 1982.
97. Aikin, A.C., J.R. Herman, E.J. Maier, and C.J. McQuillan, Influence of peroxyacetyl nitrate (PAN) on odd nitrogen in the troposphere and lower stratosphere, *Planet. Space Sci.*, 31, 1075-1082, 1983.
98. Kasting, J.F., and H.B. Singh, Nonmethane hydrocarbons in the troposphere: impact upon the odd hydrogen and odd nitrogen chemistry, *J. Geophys. Res.*, 91, 13,229-13,256, 1986.
99. Singh, H.B., and J.F. Kasting, Chlorine-hydrocarbon photochemistry in the marine troposphere and lower stratosphere, *J. Atm. Chem.*, 7, 261-285, 1988.